Applied Surface Science 464 (2019) 388–395

Contents lists available at ScienceDirect

Applied Surface Science

journal homepage: www.elsevier.com/locate/apsusc

Full Length Article

Enhanced visible-light photocatalytic CO_2 reduction performance of $ZnIn_2S_4$ microspheres by using CeO_2 as cocatalyst

Chao Yang[1], Qin Li*,[1], Yang Xia, Kangle Lv*, Mei Li

Key Laboratory of Catalysis and Materials Science of the State Ethnic Affairs Commission & Ministry of Education, Hubei Province, South-Central University for Nationalities, Wuhan 430074, PR China

ARTICLE INFO

Keywords:
$ZnIn_2S_4$
CeO_2
Cocatalyst
CO_2 reduction
Photocatalysis

ABSTRACT

$ZnIn_2S_4$ flower-like microspheres decorated with CeO_2 as cocatalyst have been successfully fabricated through a microwave-assisted hydrothermal method for visible-light carbon dioxide (CO_2) photoreduction to produce methanol (CH_3OH). All the composite photocatalysts exhibited a more excellent photocatalytic performance than bare CeO_2 and ZIS, and reached the highest with a CH_3OH evolution rate of 0.542 μmol g^{-1} h^{-1} when the content of CeO_2 was 5 wt%. In the composites, the CeO_2 with oxygen vacancies acted as a significant cocatalyst to efficiently trap the photogenerated electrons from ZIS and thus boosted the separation of photoinduced charge carriers, while the unique 3D structure of ZIS made it with a relatively large specific area, which could provide abundant active reaction sites and render the reactants and products diffuse more easily. This study verified the CeO_2 as one of the ideal cocatalyst candidates for $ZnIn_2S_4$ in the application of photocatalytic CO_2 reduction, and gave rise to an increasing interest in expanding potential applications of $ZnIn_2S_4$ based materials in the field of energy conversion.

1. Introduction

The ever-increasing carbon dioxide (CO_2) derived from excessive depletion of fossil resource has incurred numerous adverse consequences, such as greenhouse effect and energy crisis, which hinder the sustainable development of the human community [1]. It is taken into account that generation of add-value chemical fuels from CO_2 by utilizing renewable solar energy is a promising strategy to alleviate environmental challenges and energy shortage, and this research item has been attracting people's flourishing interest [2–6]. Photocatalytic reduction of CO_2 could produce various products such as methanol (CH_3OH), formic acid (HCOOH), methane (CH_4), carbon monoxide (CO), and so on [7–9]. Among them, CH_3OH is a very important and widely-used raw material in modern chemical and pharmaceutical industry applications [10]. To date, a variety of semiconductors including $ZnIn_2S_4$ [2,3,11], ZnO [12–15], TiO_2 [16–25], CdS [26,27], WO_3 [28,29], g-C_3N_4 [30–34], $CeTiO_4$ [35], $SrTiO_3$ [36], Bi_2MoO_6 [37], and SnO_2 [38,39] have been utilized for photocatalytic CO_2 photoreduction. Among them, $ZnIn_2S_4$ (ZIS) have been paid extensive attention on account of its unique structure, excellent response to visible light and suitable band structure [2,11,40]. Nevertheless, single-phase ZIS usually suffered from a rapid recombination of electron-hole pairs [41], contributing to a relatively short lifetime of photogenerated electrons, which severely oppressed the photocatalytic performance. To solve this problem, various approaches have been put forward in recent years to enhance the photocatalytic CO_2 reduction efficiency of ZIS, such as defect engineering [3], morphological control [42], and heterojunction construction [2,11]. For example, Jiao et al. proposed defect-induced electron-hole separation in ultrathin ZIS layers to achieve boosted CO_2 photoreduction efficiency [3]. Chen et al. prepared $ZnIn_2S_4$ nanosheets through a liquid ultrasonic exfoliation method, which exhibited much higher reactivity for CO_2 reduction than hydrothermally synthesized $ZnIn_2S_4$ microspheres [42]. Wang et al. [2] and Yang et al. [11] respectively fabricated well-designed ZIS-In_2O_3 hierarchical tubular heterostructures and ZIS nanosheets/TiO_2 nanobelts Z-scheme photocatalysts for efficient CO_2 photoreduction. However, to the best of our knowledge, very few reports focused on the method of cocatalyst decoration to improve the photoefficiency of ZIS in the CO_2 reduction applications.

In fact, thanks to the anisotropy growth tendency of hexagonal $ZnIn_2S_4$, it prones to form nanosheets and further self-assembled into a flower-like microsphere [43]. Such unique structure renders ZIS to be a promising supporting matrix of cocatalyst materials, which is beneficial to the enhanced separation efficiency of photoinduced carriers in the

---

* Corresponding authors.
E-mail addresses: liqin0518@mail.scuec.edu.cn (Q. Li), lvkangle@mail.scuec.edu.cn (K. Lv).

[1] Chao Yang and Qin Li contributed equally to this work.

https://doi.org/10.1016/j.apsusc.2018.09.099
Received 23 August 2018; Received in revised form 10 September 2018; Accepted 11 September 2018

photocatalytic process [44]. Therefore, choosing matched cocatalyst candidates for ZIS in the application of photocatalytic CO_2 reduction is a promising research subject.

As a nontoxic and inexpensive rare earth material, CeO_2 began to garner attention in the photocatalysis fields in recent years because of its high oxygen storage capacity and oxygen vacancy, and it has been intensively adopted in various applications, such as photoreduction of CO_2 [31], environmental decontamination [45–47], and photocatalytic H_2 production [48]. The oxygen vacancy on the surface of CeO_2 can not only enhance its light absorption ability in the visible region [49], but also promote the CO_2 adsorption and activation in the photocatalysis process [50]. More importantly, considering that sulfur atoms have similar chemical properties with oxygen atoms, the precursor of ZIS might occupy the oxygen vacancy on the surface of CeO_2, in favor of forming the compact contact between the ZIS and CeO_2 [51–53]. In addition, the reported band structure of CeO_2 in literatures is matchable with that of ZIS and meet the thermodynamic requirements of CO_2 reduction reactions [54].

Based on the above information, we novelly designed and synthesized the CeO_2 nanocube-decorated ZIS microspheres for CO_2 photoreduction in this work. It was found that the separation efficiency of photogenerated charge carriers of ZIS was immensely facilitated with the introduction of CeO_2 as a cocatalyst. The obtained composites displayed a markedly higher photocatalytic performance than bare ZIS and CeO_2. Based on series of characterization experiments, the reasons for the enhanced photoactivity of the composites were represented, and a rational reaction mechanism of the CO_2 photoreduction over the $CeO_2/ZnIn_2S_4$ composite was also proposed.

2. Experimental

2.1. Fabrication of CeO_2 nanocubes

CeO_2 nanocubes were obtained on the grounds of a previously reported approach [55]. In a typical synthetic process, $Ce(NO_3)_3 \cdot 6H_2O$ (0.87 g) was dissolved in NaOH solution (40 mL, 6 M) and stirred for 30 min to attain a homogeneous liquid. Then the liquid was poured into the Teflon liner with a capacity of 100 mL, which was sealed in a stainless steel autoclave and heated at 180 °C for 24 h, and then naturally cooled down to room temperature. The acquired white solid was separated via filtration and washed with distilled water until the pH value of the filtrate was around 7, then desiccated at 60 °C for the whole night to attain the CeO_2 precursor. Lastly, the CeO_2 precursor was put into a crucible without a cover and calcinated in the muffle furnace at 450 °C for 3 h in air atmosphere to prepare CeO_2 nanocubes, with the heating rate of 5 °C min^{-1}.

2.2. Synthesis of $CeO_2/ZnIn_2S_4$ composites

The $CeO_2/ZnIn_2S_4$ composites were prepared by a microwave-assisted hydrothermal treatment. In a typical fabrication procedure, $ZnCl_2$ (136.3 mg), $InCl_3 \cdot 4H_2O$ (586.6 mg), and thioacetamide (TAA, 601.0 mg) were dissolved in 27 mL ethanol solution ($V_{ethanol}:V_{water} = 1:2$), then various amount of the prepared CeO_2 (4.3, 21.2, 29.7, 42.3, and 84.6 mg) was added into the solution. After stirred and sonicated for 30 min, the homogeneous mixture was moved into a Teflon liner (50 mL) and kept at 180 °C for 2 h under a microwave-assisted hydrothermal treatment. After being cooled down to the ambient temperature, a yellow precipitate was obtained by the way of filtration and rinsed by distilled water and absolute ethanol for several times to make the pH value of filtrate be around 7. At last, the product was desiccated at 70 °C for 2 h in a vacuum oven. The obtained samples were denoted as CZx (x = 1, 5, 7, 10, and 20, respectively), where x represented the theoretical mass percentage of CeO_2 to $ZnIn_2S_4$. For comparison, pure $ZnIn_2S_4$ was synthesized with a same approach in the absence of CeO_2 cubes, named as ZIS.

2.3. Photocatalytic CO_2 reduction

All of the prepared photocatalysts were degassed at 150 °C for 6 h prior to the measurements. Specifically, a Xe lamp (300 W, XD 350, CHINA) equipped with an UV-cutoff filter ($\lambda \geq 420$ nm) was exploited as the visible-light source. The degassed samples (100 mg) and $NaHCO_3$ (84 mg) were individually added into a two-neck Pyrex reactor possessing two parallel planes, which was sealed by a rubber stopper. Later, the reaction system was purified using N_2 for one hour to totally eliminate air. H_2SO_4 was carefully immitted into the special groove on one neck of the reactor to react with $NaHCO_3$, so that CO_2 was in-situ generated in this closed system. The resulting gas (1 mL) was injected by the syringe, and then detected and analyzed in virtue of gas chromatography (GC-14C, SHIMADZU, JAPAN) at an interval of one-hour irradiation.

3. Results and discussion

3.1. Phase structure

X-Ray diffraction (XRD) patterns were analyzed to determine the crystallographic structure of synthesized photocatalysts. From the XRD patterns shown in Fig. 1a, spiculate peaks of the pure CeO_2 can be observed at 28.6°, 33.2°, 47.6°, and 56.4°, respectively indexed to the (1 1 1), (2 0 0), (2 2 0), and (3 1 1) facets of CeO_2 with a cerianite phase (JCPDS, No. 34-0394) [48]. In the XRD pattern of bare ZIS, the diffraction peaks located at 27.7°, 30.5°, and 47.2° are respectively ascribed to (1 0 2), (1 0 4), and (1 1 0) facets of the hexagonal-phase ZIS (JCPDS, No. 65-2023) [40]. In the composites, when the mass fraction of CeO_2 was less than 10 wt%, the XRD peaks of CeO_2 were not observed obviously. With the augment of the CeO_2 loading amount, the intensity of the diffraction peaks of CeO_2 increased, which can be clearly viewed from partial-amplificatory XRD pattern of its (1 1 1) facet (Fig. 1b). In addition, the characterized peaks of CeO_2 in the composites exhibited an evident skewing to the lower angle. It suggests that a robust interaction was formed between CeO_2 and ZIS. These results preliminarily demonstrated the fact that $CeO_2/ZnIn_2S_4$ composite photocatalysts were well fabricated as expected.

3.2. Morphology

Field emission scanning electron microscopy (FESEM) and transmission electron microscopy (TEM) images were recorded to directly observe the morphologies of CeO_2 and ZIS and their interposition relationships in the composites. Fig. 2a shows that CeO_2 possesses a cubic morphology with the size ranging from 50 to 500 nm, whilst Fig. S1a shows that ZIS adopts a 3D hierarchical flower-like structure assembled by 2D nanosheets with several micrometers in diameters. In the CZ5 sample, CeO_2 nanocubes gleamingly interspersed in the ZIS

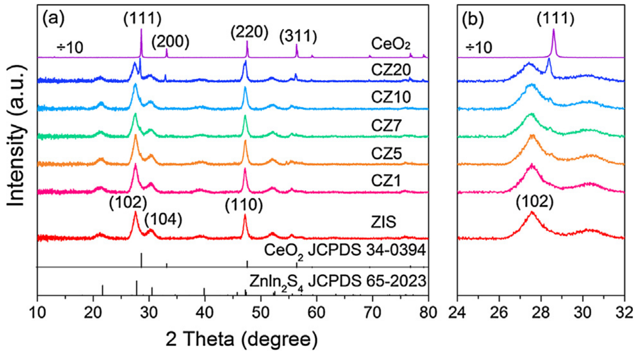

Fig. 1. (a) XRD patterns and (b) partial-amplificatory patterns of the prepared samples.